Available online at www.sciencedirect.com
SCIENCE DIRECT®
PERGAMON
Solid-State Electronics 46 (2002) 2291–2294
SOLID-STATE ELECTRONICS
www.elsevier.com/locate/sse

Investigation of radiative tunneling in GaN/InGaN single quantum well light-emitting diodes

X.A. Cao [a,*], S.F. LeBoeuf [a], K.H. Kim [b], P.M. Sandvik [a], E.B. Stokes [a], A. Ebong [a], D. Walker [a], J. Kretchmer [a], J.Y. Lin [b], H.X. Jiang [b]

[a] GE Research Center, One Research Circle, KWC 1403, Niskayuna, NY 12309, USA
[b] Department of Physics, Kansas State University, Manhattan, KS 66506, USA

Received 28 March 2002; accepted 12 April 2002

Abstract

The mechanisms of carrier injection and recombination in a GaN/InGaN single quantum well light-emitting diodes have been studied. Strong defect-assisted tunneling behavior has been observed in both forward and reverse current–voltage characteristics. In addition to band-edge emission at 400 nm, the electroluminescence has also been attributed to radiative tunneling from band-to-deep level states and band-to-band tail states. The approximately current-squared dependence of light intensity at 400 nm even at high currents indicates dominant nonradiative recombination through deep-lying states within the space-charge region. Inhomogeneous avalanche breakdown luminescence, which is primarily caused by deep-level recombination, suggests a nonuniform spatial distribution of reverse leakage in these diodes.

Keywords: Light-emitting diode; GaN; Radiative tunneling; Nonradiative recombination

1. Introduction

III–V nitrides involving Ga, Al and In have attracted much attention in the past decade due to the emerging applications for blue and ultraviolet optoelectronic devices [1,2]. Owing to the lack of a lattice-matched substrate, GaN and its alloys are most commonly grown heteroepitaxially by metalorganic chemical vapor deposition (MOCVD) on sapphire. As-grown films are known to contain a high density of threading dislocations traversing vertically from the epilayer/substrate interface to the epilayer surface, due to the large lattice mismatch and thermal expansion coefficient difference between GaN and sapphire [3,4]. In contrast to GaAs-based optical emitters, where a dislocation density of 10^4 cm^{-2} is sufficient to prevent laser operation [4], GaN-based light-emitting diodes (LEDs) and laser diodes work efficiently despite high dislocation densities (10^8–10^{10} cm^{-2}). One common explanation to this controversy is that threading dislocations do not contribute to electronic states in the bandgap of GaN, or bandgap states associated with dislocations are not electrically active. This assumption was supported by previous calculations [5] and experimental results [6]. On the other hand, there is also experimental evidence that dislocations in III-nitrides are nonradiative recombination centers [7,8]. Results from a recent scanning capacitance microscopy study suggest that negative charges exist near dislocations [9], and calculations show that these negatively charged defects may scatter the carriers, and introduce deep-level states [10,11]. The threading dislocations can also contribute to deep-level states or band tails due to the dangling bonds at Ga and N atoms located along or close to the dislocation core [12].

In addition to the dislocations, other possible candidates for the bandgap states in III-nitrides include structural defects such as grain boundaries [13], and nitrogen or gallium vacancies [14,15], or impurities such

* Corresponding author. Fax: +1-518-387-5997.
E-mail address: cao@crd.ge.com (X.A. Cao).

0038-1101/02/$ - see front matter
PII: S0038-1101(02)00190-9

as oxygen [15], carbon [16] or hydrogen complexes [17]. It is important to understand the effects of these defect states on the electrical and optical properties of light-emitting devices, since they could act as recombination channels and as carrier traps that result in a decrease in carrier lifetime and emission efficiency. In this study, we have observed strong tunneling behavior in GaN-based LEDs with an InGaN single quantum well (SQW) active region. Radiative and nonradiative recombination involving bandgap states in the space-charge region indicate the electrical and optical activity of defects in III-nitride materials.

2. Experimental

The LED wafers were grown on sapphire (0 0 0 1) substrates with a 30 nm GaN buffer layer by low-pressure MOCVD. The device structure consists of a 3.5 μm Si-doped GaN, a 0.1 μm Si-doped superlattice consisting of alternating layers of AlGaN (5 nm)/GaN (5 nm), a 3 nm undoped InGaN active layer, followed by 14 periods of Mg-doped AlGaN (5 nm)/GaN (5 nm) superlattice, and a 0.5 μm Mg-doped GaN epilayer. The wafer was then annealed at 950 °C for 10 s in nitrogen. This process produced room temperature p-doping and n-doping concentrations of 5×10^{17} and 2×10^{18} cm^{-3}, respectively. Fig. 1 shows an AFM image of a 1 μm^2 region from the original epitaxial surface. The density of the small pits ($\sim 3 \times 10^9$ cm^{-2}) has consistently been found to be comparable to the density of dislocations which thread through the entire epilayer and intersect the top surface, as determined by cross-sectional transmission electron microscopy. In order to fabricate the LED devices, the p-GaN was partially etched to form mesas of 300×300 μm^2 squares using an inductively coupled plasma etching system. Ni/Au and Ti/Al were deposited by electron beam evaporation, and followed by a 550 °C anneal to form p-type and n-type ohmic contacts, respectively.

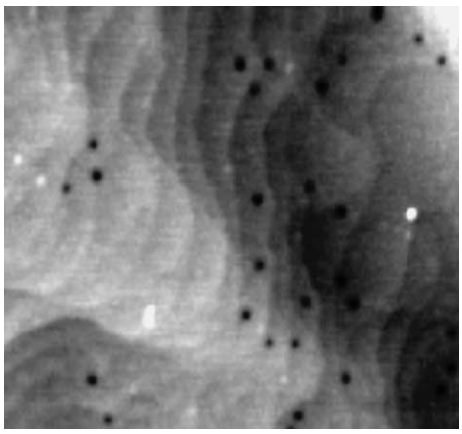

Fig. 1. AFM image of typical surface region (1 μm^2) of the GaN/InGaN SQW LED samples.

3. Results and discussion

Fig. 2 shows a series of forward current–voltage (I–V) characteristics of the LEDs measured at increasing temperatures ranging from 20 to 200 °C. At moderate biases (1.9–2.7 V), the current does not follow kT or $2kT$ slopes, but the I–V behavior can be described by $I = I_0 \exp(qV/E)$. The energy parameter E has a value of 105 meV, and does not depend on temperature. The extracted unrealistic ideality factor of 4, and the temperature independence of the parameter E, are typical features of tunneling conduction in a p–n junction [18]. The current component with an energy parameter of $\sim$105 meV has been associated with holes tunneling into the InGaN QW region with involvement of deep acceptor states [19]. The excess current could also result from a more complex process involving multiple-step tunneling-recombinations. This could occur in these diodes because of the presence of a high-density of microstructural defects. Similar defects are also believed to be responsible for some deep-level states associated with the mid-gap yellow luminescence band [15], which is observed in the photoluminescence of our samples. The reverse leakage currents in the LEDs are much higher than the classical diffusion and generation-recombination currents, and weakly temperature-dependent. This is another indication of the presence of tunneling current. Defect-assisted tunneling was also found to be responsible for the current transport in most commercially available blue and green emitters [20]. In our previous

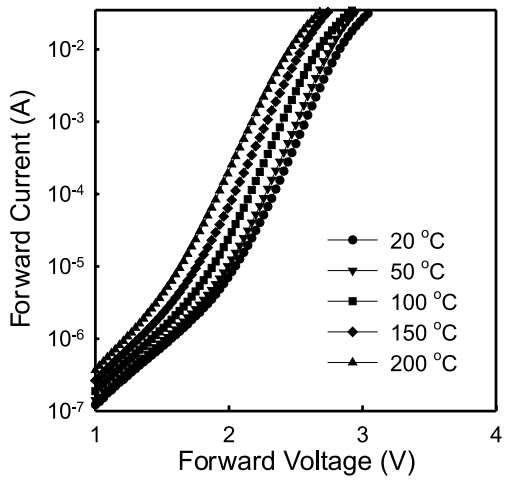

Fig. 2. Forward I–V characteristics of the GaN/InGaN SQW LEDs measured at 20–200 °C.

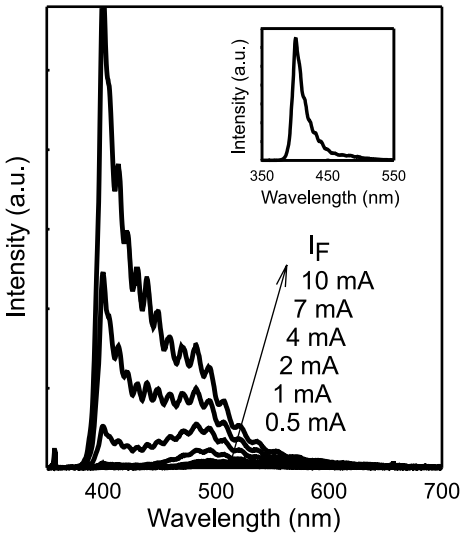

Fig. 3. EL spectra of the GaN/InGaN SQW LEDs at increasing forward current. (The EL spectrum at 100 mA is shown in the inset.)

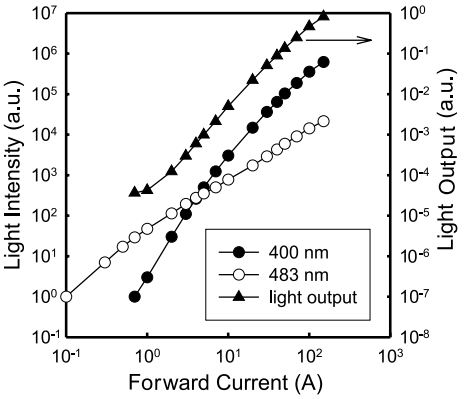

Fig. 4. The dependence of overall light output, and light intensity at 483 and 400 nm on the forward current of the GaN/InGaN LEDs.

work, we observed dominant temperature-dependent diffusion-recombination process in a high quality GaN/InGaN multiple quantum well LED, where the defect density in the space-charge region was substantially reduced [20].

Fig. 3 shows the electroluminescence (EL) spectra of the LEDs at increasing forward current. At currents less than 2 mA, only deep-level emission with a single peak at ~483 nm is observed. This is evidence that carriers tunnel into the deep-level states in the InGaN active region followed by radiative recombination. The position of the major deep-level states is about 0.54 eV from the energy-band of InGaN. With the increase of current, a separate sharp peak at 400 nm associated with the InGaN band-edge transition appears. In the meantime, the gradual band-tail luminescence becomes more and more significant. The rapid growth of the band-edge emission as well as the band-tail emission, as shown in Fig. 3, indicates the dramatic increase of tunneling flux to the corresponding bands. In the low injection regime, carrier tunneling to deep-level states may dominate, leading to the generation of defect luminescence with negligible band-edge emission. Upon increasing forward bias, the probability for electrons to inject to the band-tail states and the InGaN energy-bands increases, leading to a substantial increase of the transition rate from band-to-band and band-to-tail states. The InGaN band-edge EL dominates at high currents, as can be seen in the inset of Fig. 3.

Fig. 4 shows the evolution of total light output and intensity of the 483 nm peak and the 400 nm peak. The total output and intensity of band-edge emission are approximately current-squared dependent, indicating nonradiative recombination. While we observed radiative emission associated with deep-level states, the current transport through the p–n junction may be dominated by nonradiative tunneling via one or multiple bandgap states. On the other hand, the intensity of the 483 nm peak is nearly linear, following the forward current. This suggests that the radiative tunneling may be limited by the tunneling rate of carriers to the deep-level states. As can be seen in Fig. 3, the nonradiative recombination centers are not saturated even at high currents, suggesting strong optical activity of the defects in these devices. This is in a sharp contrast to commercial GaN/InGaN MQW LEDs, where we found saturation was reached at a current densities as low as 1.4×10^{-2} A/cm^2 [20]. The discrepancy may be partly attributed to the poorer quality of the interface between the active layer and the cladding layer with a higher Al ratio, and reflects the epitaxial growth challenges facing efficient violet emitters. The relatively low quantum efficiency in these LEDs may also result from nonoptimized InGaN growth. It is well accepted that In segregation in InGaN can localize the injected carriers and prevent carrier recombination at structural defects including dislocations. Differences in localization effects may also partially explain the wide spread in quantum efficiencies in the commercial blue and green LEDs.

The breakdown luminescence spectra at −5 and −10 mA for the LEDs are shown in Fig. 5. The overall intensity is several orders of magnitude lower than that of forward injection luminescence. In this case, the devices are under moderate reverse biases ($V < -10$ V). Strong band-to-band tunneling occurs due to high doping concentrations on both sides of the p–n junction. Carriers drifting in the high electric field to the boundaries of the space-charge region gain sufficient energy to cause impact ionization [21]. The breakdown luminescence

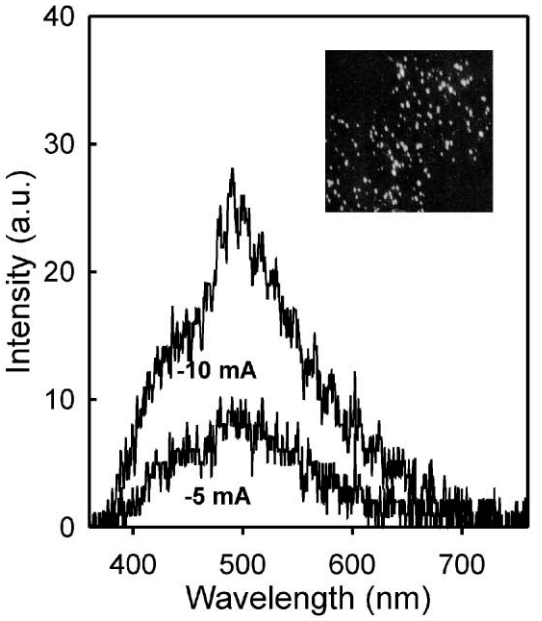

Fig. 5. Avalanche breakdown luminescence of the LEDs at −5 and −10 mA. (The LED microphotograph at −10 mA is shown in the inset.)

results from radiative recombination of a small portion of these generated electron–hole pairs. The broad band of the luminescence shown in Fig. 5 indicates that recombination via defect states dominates. The high-energy edges of the spectra are at the band-edge of the InGaN rather than the GaN, suggesting negligible band-to-band recombination in the GaN cladding layers. It is striking that the luminescence is strongly localized at some particular regions (see the inset of Fig. 5), with a density of the emission spots of $\sim 10^6$ cm^{-2} readily identified by the naked eye. This is indicative of inhomogeneous spatial distribution of reverse leakage currents in these devices. In the areas with high density of structural defects, the electric field, and therefore the impact ionization rate, are much higher, resulting in much higher leakage densities. Nonuniform currents were also reported in GaN Schottky diodes, where the reverse leakage was found to occur primarily at microstructural defects such screw dislocations [22].

4. Conclusions

In conclusion, we have observed significant influence of microstructural defects on the electrical characteristics and optical efficiency of GaN/InGaN SQW LEDs. Radiative and nonradiative tunneling has been found to be responsible for the current transport across the p–n junction. Inhomogeneous avalanche breakdown luminescence indicates that reverse leakage currents are concentrated in the areas with high-density defects. Our study shows that a significant number of defects in GaN-based materials are electrically and optically active. Understanding the origin and nature of these defects, and minimizing the defect formation during epitaxy will be an important endeavor in the near future for improvement of efficiency of III-nitride-based emitters.

References

[1] Nakamura S, Mukai T, Senoh M. Appl Phys Lett 1994;64:1687.
[2] Akasaki I, Sota S, Sakai H, Tanaka T, Koike M, Amano H. Electron Lett 1996;32:1105.
[3] Heying B, Wu XH, Keller S, Li Y, Kapolnek D, Keller BP, et al. Appl Phys Lett 1996;68:643.
[4] Ponce FA, Cherns D, Young WT, Steeds JW. Appl Phys Lett 1997;69:770.
[5] Elsner J, Jones R, Sitch PK, Porezag VD, Elstner M, Frauenheim T, et al. Phys Rev Lett 1997;79:3672.
[6] Vertikov A, Kuball M, Nurmikko AV, Chen Y, Wang SY. Appl Phys Lett 1998;72:2645.
[7] Ronser SJ, Carr EC, Luydowise MJ, Girolami G, Erikson HI. Appl Phys Lett 1997;70:420.
[8] Hino T, Tomiya S, Miyajima T, Yanashima K, Hashimoto S, Ikeda M. Appl Phys Lett 2000;76:3421.
[9] Hansen PJ, Strausser YEW, Erickson AN, Tarsa EJ, Kozodoy P, Brazel EG, et al. Appl Phys Lett 1998;72:2247.
[10] Look DC, Sizelove JR. Phys Rev Lett 1999;82:1237.
[11] Leung K, Wright AF, Stechel EB. Appl Phys Lett 1999;74:2495.
[12] Lee SM, Belkhir MA, Zhu XY, Lee YH. Phys Rev B 2000;61:16033.
[13] Ponce FA, Bour DP, Gotz W, Wright PJ. Appl Phys Lett 1996;68:57.
[14] Neugebauer J, VandeWalle CG. Appl Phys Lett 1998; 69:503.
[15] Elsner J, Jones R, Heggie MI, Oberg S, Briddon PR. Phys Rev B 1998;58:12571.
[16] Ogino T, Aoki M. Jpn J Appl Phys 1980;19:2395.
[17] Brandt MS, Johnson NM, Molnar RJ, Singh R, Moustakas TD. Appl Phys Lett 1994;64:2264.
[18] Dumin DJ, Pearson GL. J Appl Phys 1965;36:3418.
[19] Perlin P, Osinski M, Eliseev PG, Smagley VA, Mu J, Banas M, et al. Appl Phys Lett 1996;69:1680.
[20] Cao XA, Stokes EB, Sandvik P, LeBoeuf SF, Kretchmer J, Walker D. IEEE Electron Device Letters.
[21] Sze SM. Physics of semiconductor devices. 2nd ed.. 1981.
[22] Hsu JWP, Manfra MJ, Lang DV, Richter S, Chu SNG, Sergent AM, et al. Appl Phys Lett 2001;78:1685.